Theor. Appl. Climatol. 69, 103–122 (2001)

Theoretical and Applied Climatology

© Springer-Verlag 2001
Printed in Austria

[1] The Department of Geography, The Hebrew University of Jerusalem, Israel
[2] The Open University of Israel, Tel Aviv, Israel
[3] Earth Science Institute, The Hebrew University of Jerusalem, Israel
[4] Soil Erosion Research Station, Ministry of Agriculture, Israel

A severe autumn storm over the middle-east: synoptic and mesoscale convection analysis

U. Dayan[1], **B. Ziv**[2], **A. Margalit**[3], **E. Morin**[3,4], and **D. Sharon**[3]

With 19 Figures

Received July 4, 2000
Revised January 16, 2001

Summary

At times, a pronounced trough of low barometric pressure extends from equatorial Africa northward, over the Red Sea and the eastern Mediterranean countries, i.e., the Red Sea Trough. The associated weather is usually hot and dry, and consequently the atmosphere becomes conditionally unstable. In cases in which additional moisture is supplied and dynamic conditions become supportive, as the case analyzed here, intense thunderstorms occur, with extreme rain rates, hail and floods.

The storm herein analyzed caused extensive damage both in casualties and property and evolved in two main consecutive phases: In the first a Mesoscale Convective System that moved from Sinai northward over Israel dominated, and in the second deep convection was organized mainly along a cold front.

Data analysis indicates several synoptic-scale factors that had a supportive effect on the storm formation and intensification: Conditional instability established by the Red Sea trough, mid-level moisture transport from Northern Africa, and upper-level divergence imparted by both polar and subtropical jet streams over the Middle-East.

Mesoscale features were further investigated by means of a hydro-meteorological observational analysis with high spatio-temporal resolution using raingauge and radar data, and satellite imagery. It is shown that local factors, particularly topographic effects, play a major role in the evolution, intensity and spatial organization of the convective activity.

Our findings support results of a numerical study of another autumn rainstorm associated with the Red Sea trough. In the present case we identify an additional contributing factor, i.e., a mid-latitude upper-level trough that further intensified the storm as it was approaching the Middle-East.

1. Introduction

An intense rainstorm struck the Middle-East (ME) between 17 and 19 October 1997. The storm, with its associated showers, caused extensive damages both in casualties and infrastructure. At least 6 people were killed in Egypt and 9 in Israel. In Jordan, 2 people were drowned by floods in the vicinity of Amman (Fig. 1).

Torrential rain and thunderstorms with huge hail stones (2.5–5.0 cm diameter, see Sec. 5 below) and gusty winds swept parts of Israel. Rain intensities exceeded $100\,\mathrm{mm\,h^{-1}}$ for 10 minutes which in Jericho, for instance, has a return period of over 30 years (Morin et al., 1998). Extreme floods were observed, especially in small arid watersheds (less than $300\,\mathrm{km^2}$). In some cases record values of peak discharge were registered, such as $4\,\mathrm{m^3\,s^{-1}}$ in a $0.5\,\mathrm{km^2}$ watershed near Eilat (Schick, personal communication) and $160\,\mathrm{m^3\,s^{-1}}$ in a $36\,\mathrm{km^2}$ watershed east of Beersheba (Garti, personal communication). Flash floods caused the drowning of 3 children and a woman in the northern Negev, 5 other people were killed and

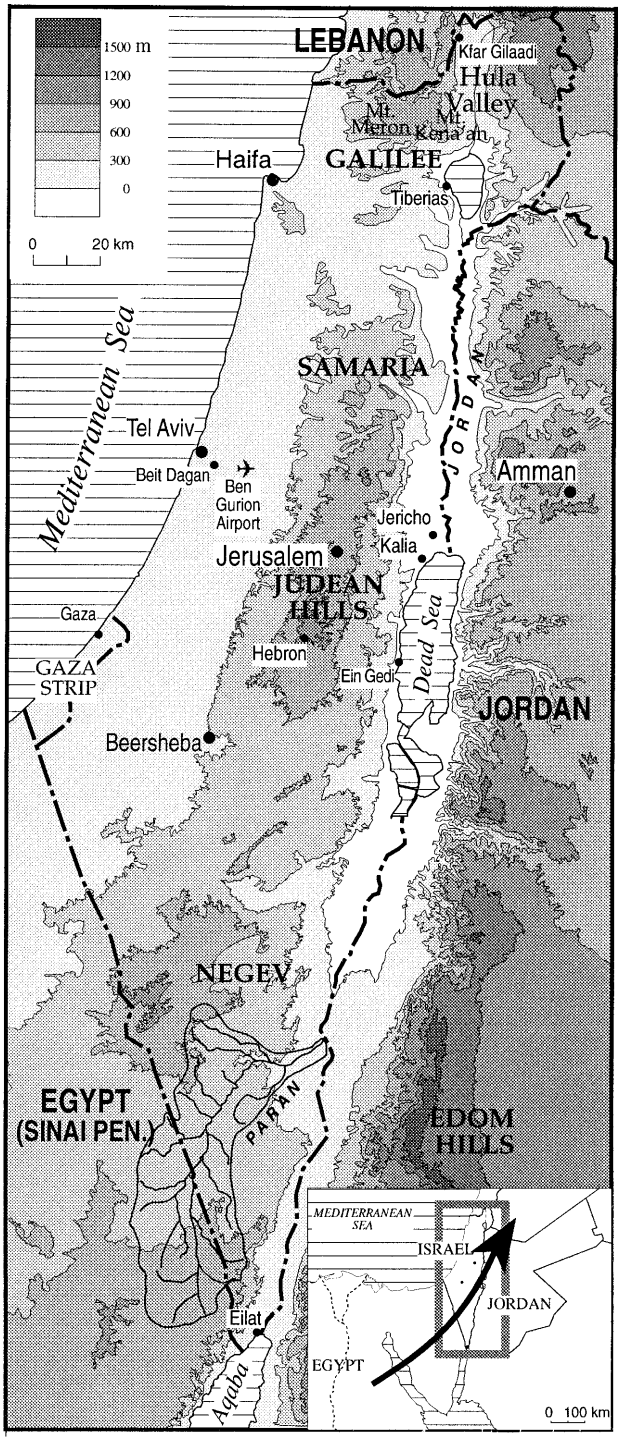

Fig. 1. Location map – Progression of the rainstorm over the Middle-East during the 17 and 18 October 1997. The arrow represents the movement of the Mesoscale Convective System on the 17 October 1997

over 50 people were rescued from several creeks in the Judean desert. Several roads and protective devices were damaged by floods, causing, among others, the closing of Eilat airport for 24 hours and the flooding of a school, luckily during school vacation.

Localized convective showers are common in the ME in the fall. In the arid southern part of Israel (the Negev) they contribute 15–25% of the annual rainfall in the form of high intensity rains exceeding 30 mm h^{-1} (Sharon and Kutiel, 1986). In lower-latitude subtropical deserts showers of this type are the major rainfall source (Sharon, 1974, 1981; Krichak et al., 1997a).

The occurrence of such rainstorms in the study area has been attributed mainly to intrusions of a low-pressure trough extending from Sudan toward the ME, i.e., the Red Sea trough (Ashbel, 1938; El-Fandi, 1948). This trough is a dominant feature in the ME in October (Bar-Lavy et al., 1977; Dayan and Sharon, 1980; Ronberg, 1985), and is regarded as an extension of the African Monsoon (El-Fandi, 1948).

The annual climatic regime of the African Monsoon trough is controlled by the converging trade winds in the ITCZ, which oscillates (at 0° longitude) between 5–10° N in the winter and 20–25° N in the summer (Hayward and Oguntoyimbo, 1987). Its normal position for October is 15–20° N, over the heated continental interiors of central and East Africa (Barry and Chorley, 1998).

Three consecutive stages can be discerned in the course of the episode treated below: Antecedent conditions and two phases of the storm itself. Prior to the onset of the storm a Red Sea trough extended over the Levant region and transported hot and dry air from the Arabian Desert at the lower levels, leading to a build-up of conditional instability throughout the troposphere. The 1st phase of the storm was dominated by a Mesoscale Convective System (MCS) that moved from Sinai northward over Israel. At the 2nd phase intense convection was organized along an approaching mid-latitude cold front that swept Israel on the following day. Thus, this storm, and others of its type that occur in this particular geographical setting, represents a special case of a tropical/extra-tropical interaction, involving elements from the African Monsoon, the subtropical jet and a mid-latitudinal cyclone. The above-mentioned convergence of phenomena from arid and marine environments, though interesting in itself, also poses a serious problem of data availability, unlike in extensive continental regions. This situation may explain why studies on rainstorms associated

with the Red Sea trough have hitherto focused on relatively narrow aspects, such as numerical studies on the dynamics and evolution of such storms (Krichak et al., 1997a,b; Krichak and Alpert, 1998) or an in depth analysis of the hydrometeorological aspects of resulted flood (e.g., Greenbaum et al., 1998).

The purpose in the present study is to gain – and present – a broader and more comprehensive perspective on observational characteristics of a storm, using various types of data that complement each other in illustrating the structure of the storm and the factors affecting its evolution in time. We, therefore, concentrate on synoptic-scale data derived from global data sources, on satellite and radar imagery, local surface observations over Israel and, in the absence of the latter, even indirect hydrological evidence on rainfall inputs. Section 2 below briefly describes the various methodologies by which the storm was analyzed. Sections 3–5 describe the evolution of each of the above mentioned stages, and concluding remarks follow in section 6.

2. Data and methodology

The fields used for the synoptic-scale analysis are taken from sets of the NCEP/NCAR reanalysis data with $2.5^\circ \times 2.5^\circ$ resolution (Kalnay et al., 1996). The upper-level soundings from Beit Dagan (see Fig. 1) and some complementary synoptic data were obtained from the Israeli Meteorological Service, the infra-red satellite imagery from the NOAA polar orbiters, and the water-vapor imagery from METEOSAT geosynchronous satellite.

Rainfall totals were derived from 350 official rain gauges (Israel Meteorological Service) and 40 Dynes autographic rainfall recorders and data loggers (Israel Meteorological Service, Hebrew University Arid Ecosystems Research Center). Data on the distribution of rain intensities in time and space were obtained through application of the software package RAIN (Morin and Sharon, 1993). The detailed analysis of the rainfall systems during the two phases of the storm was performed, using the following tools:

- maps of daily rainfall totals
- rain charts from recording stations
- isochrone maps (after Kelway and Herbert, 1969), in which isolines connect locations with equal timing of rain occurrence. To reduce irregularities, isochrones denote the time by which 15% of the daily total was accumulated.
- radar reflectivity data, as specified below

For October 17, only hourly scans were available from the meteorological radar (C-band) operated by Electro-Mechanical Service Ltd (EMS) at Ben-Gurion International Airport, 10 km south east of Tel Aviv. The range of its beam is 185 km. On October 18, 5-minute data were derived from the Tel Aviv University C-band radar with similar specifications. The data from both radar systems were obtained from beam elevations of 0.7–2.1°. The latter is equivalent to 3.25–4.35 km a.s.l. at 90 km, within which the most active cells were detected.

In the following the referenced time is UTC. Note that UTC lags behind the LST in Israel by 2 hours.

3. Antecedent conditions (Oct 14–17)

Between Oct 14 and 16 congested clouds were scattered between 7–12° N over Africa with an extension toward the southern part of the Red Sea (Fig. 2). Their location corresponded to the climatological position of the African Monsoon trough for October, i.e., several degrees south of the Monsoon trough as expected by Sadler (1975).

At the same time the Levant region was subjected to a south-easterly flow at the lower levels under the influence of the Red Sea trough (Fig. 3a). At the lower levels warm advection prevailed, resulting in a significant surface temperature rise of up to 35 °C in the inner coastal plains of Israel on October 16 (8 °C above normal, Israel Meteorological Service, 1983) and to 24 °C at the 850 hPa level (Fig. 3b, 9 °C above normal). At the same time temperatures at the higher troposphere were 2 °C to 4 °C below normal (after Shaia and Siles, 1972) at the 500 and 300 hPa levels, respectively. This differential warming enhanced static instability with respect to the normal conditions.

The soundings of Beit-Dagan (central Israel) for Oct 16 and 17 (Fig. 4a,b) indicate both conditional instability within the 900 to 400 hPa layer. During that 24 h period the relative humidity within the 900–600 hPa layer increased from 15–40% to 35–85%, while no significant change

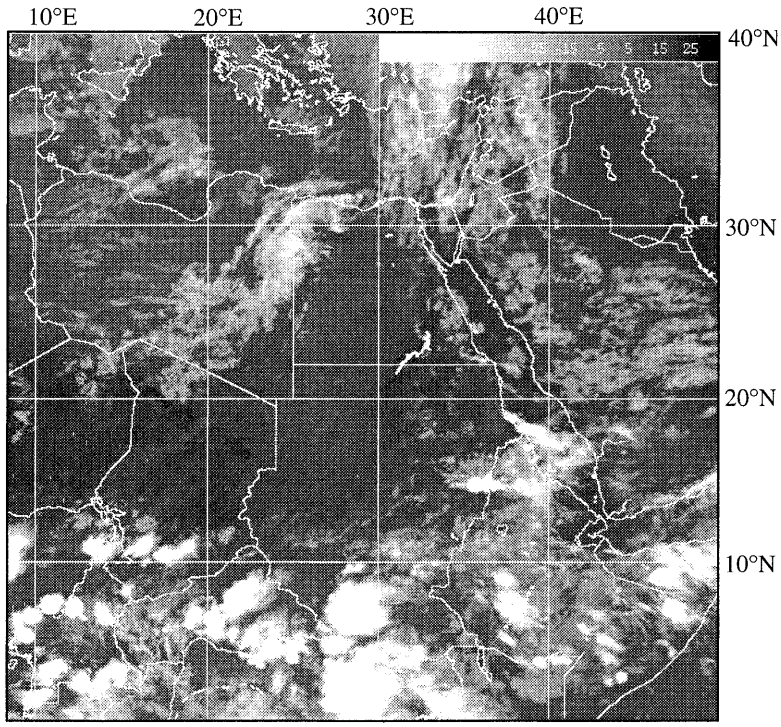

Fig. 2. NOAA satellite IR imagery for 1800 UTC 16 Oct 1997, showing the congested tropical cloud above Africa and the Red Sea (bottom)

in the temperature profile was observed. This resulted in a respective lowering of the lifting condensation level (LCL) from 610 to 705 hPa (about 1200 m). The tephigram for Oct 16 1100 UTC (Fig. 4a) indicates an inhibition of convection (for parcel lifted from 900 hPa, at the top of the lower stable layer). The Convective Available Potential Energy (CAPE) calculated for the following day (Oct 17 1100 UTC) was 1187 $J\,kg^{-1}$ (assuming lifting of parcel from 925 hPa layer up to 300 hPa, Fig. 4b). This change paved the way for the development of the deep convection that took place later. Figure 5 indicates mid-troposphere moist advection from south-west. The water vapor imageries (not shown) indicate the existence of a band of upper-atmospheric moist air with a south west-north east orientation extending from western equatorial Africa toward the ME.

The resulting cloudiness is clearly seen on the satellite imagery (Fig. 7). However, at this stage, before 17 Oct 1400 UTC, no significant rainfall was yet recorded over Israel. The bases of individual clouds are all well aligned with the main topographic ridges along the Red Sea coast, e.g. along the coastal ridge in eastern Egypt, the mountainous area of southern Sinai and over the hills of Edom in western Jordan.

4. Phase I: Mesoscale convection: synoptic scale forcing and topographic effects (Oct 17)

4.1 The onset of the storm

While the Red Sea trough dominated the ME at the lower levels, a well developed upper trough extended from eastern Europe to the Mediterranean near Greece with a northerly polar jet (PJ) to its west, over central Europe, and another PJ streak with south-south-west orientation ahead of it, over Turkey (Fig. 8a). While maintaining its zonal position, the wind speed within the subtropical jet (STJ) was larger by over 80% than its monthly normal speed (about 27 $m\,s^{-1}$, Air Ministry Meteorological Office, 1962), with a maximum of 45 $m\,s^{-1}$ over Libya.

The anvils of individual Cumulonimbi that developed over the Red Sea region south of 27° N, point toward the east north-east (Fig. 9), reflecting the upper-level winds associated with the STJ. This is more clearly seen in the visible imagery (not shown), where the core of such a cloud is brighter than its anvil. A point of diffluence (not necessarily implying divergence) between the latter and the PJ (Fig. 8b, dashed line) is uniquely reflected by the delta-shaped (60° angle) anvil of the active cell over southern Sinai.

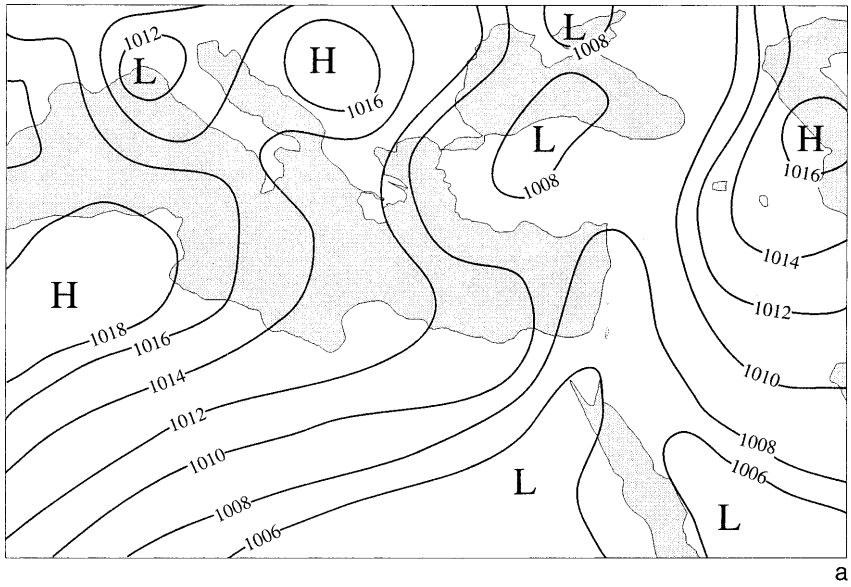

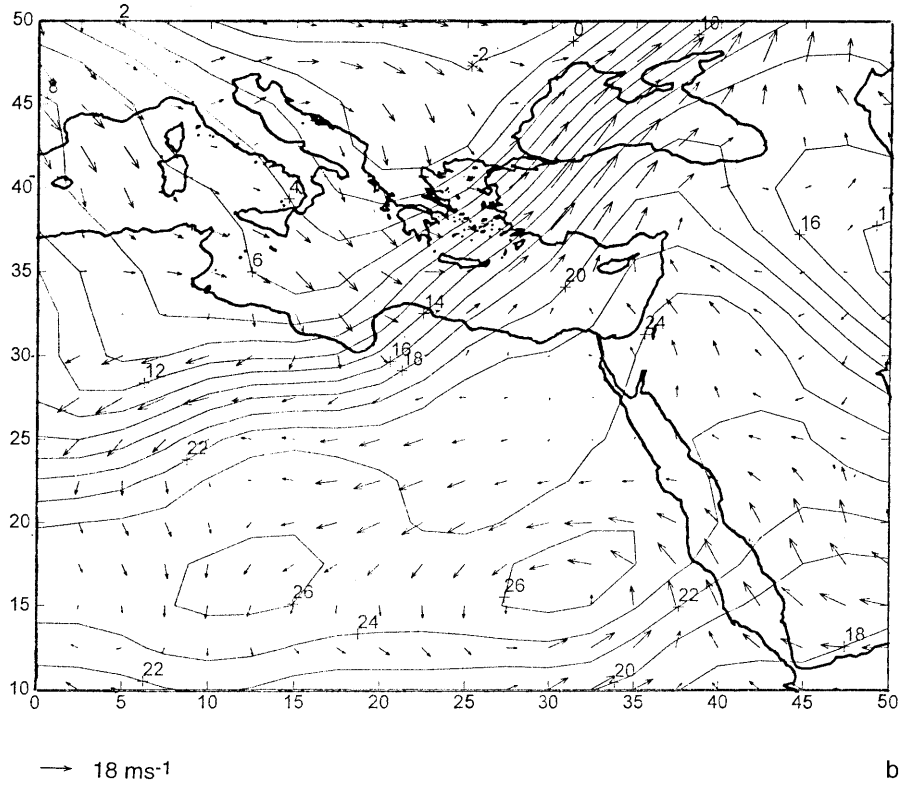

Fig. 3. Lower-level analysis for 0000 UTC 16 Oct 1997: (**a**) Sea level pressure (hPa), showing the Red Sea trough over the ME. (**b**) 850 hPa. Isotherms, with 2 °C interval, and wind vectors, showing warm advection over the Levant region

Several synoptic-scale factors are suggested as supportive for the initiation of the rainstorm:

- The lower-level convergence (Fig. 10), reflecting a combined effect of the Red Sea trough and the sea breeze.
- The 200 hPa divergence center with a maximum of over $40 \times 10^{-6}\,s^{-1}$ over the eastern part of the Mediterranean (Fig. 8b) that was proceeding toward the east (not shown).
- The mid-tropospheric moisture transport from western equatorial Africa as may be deduced from both the relative humidity and wind fields (e.g. Fig. 5) and the water vapor imagery.
- A cold advection that took place at that time over the Levant region, as seen in the lower-

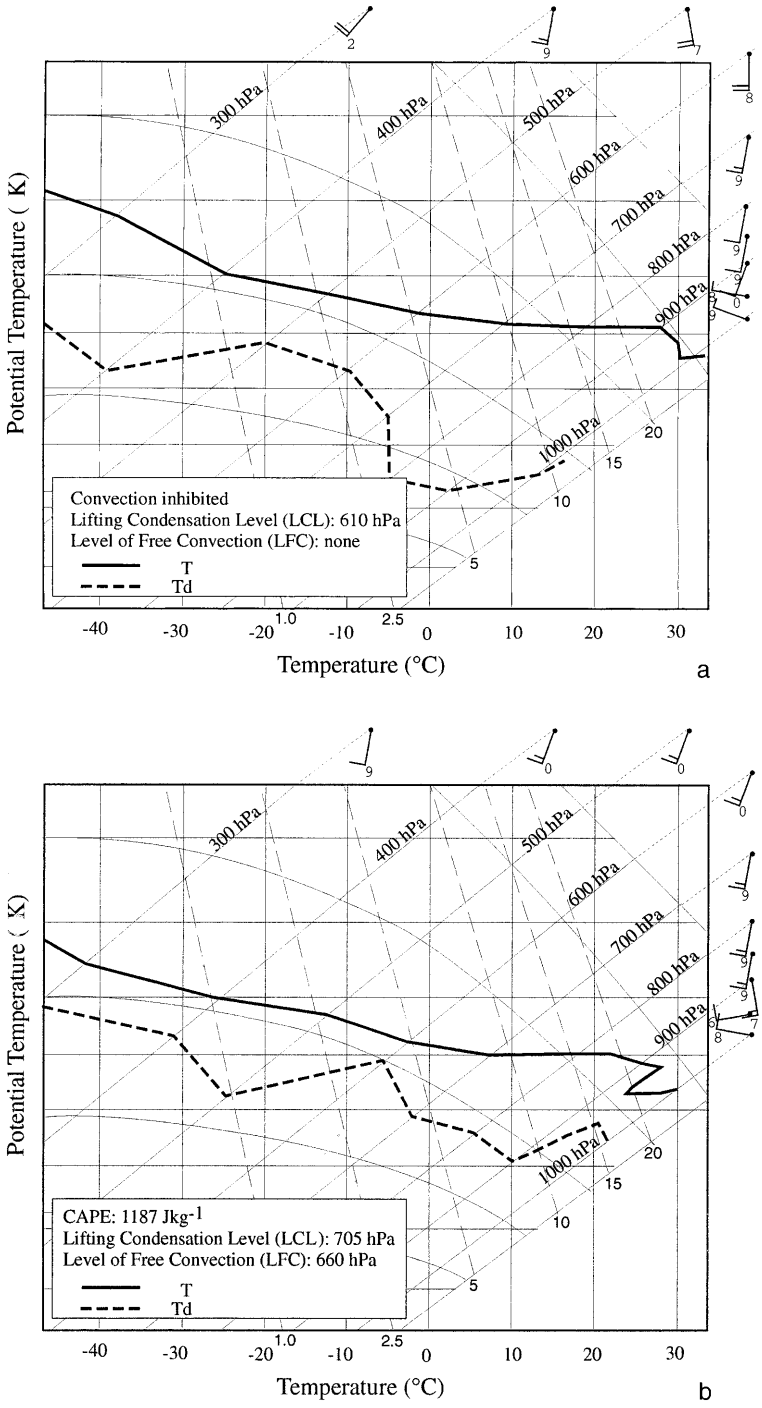

Fig. 4. Soundings from Beit-Dagan (Central Israel), containing temperature (denoted 'T') and dew point (denoted 'Td') for (**a**) 1100 UTC 16 Oct 1997, and (**b**) 1100 UTC 17 Oct 1997. Conventional wind barbs represent $5.0\,m\,s^{-1}$. Both wind profiles show a uniform south-southwesterly flow at middle and high levels, while the westerlies at the lower 1 km may be attributed to the sea breeze (the station is located 8 km inland). Note the increase in relative humidity. The term 'CAPE' means Convective Available Potential Energy

level temperature field (e.g. Fig. 6), suggesting the existence of a cold front.

The latter factors together with the combination of lower-level convergence and upper-level divergence, intrinsically linked through continuity equation to upward motion at the mid-troposphere, enhanced the potential for the initiation of intensive rain-showers where local factors were involved as specified below.

4.2 Mesoscale convection

Analyses of rainfall charts, rainfall totals, satellite and radar imagery reveal detailed information on

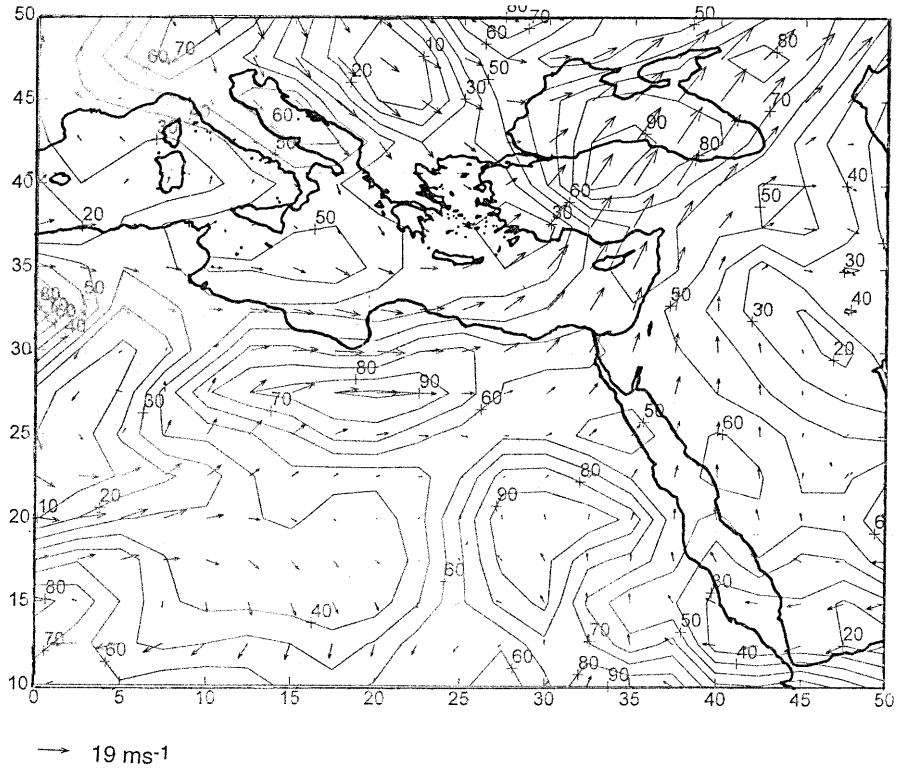

Fig. 5. Relative humidity (10% interval) and wind vectors at 700 hPa for 1200 UTC 17 Oct 1997, showing a region with high relative humidity over Libya. The wind vectors reflect that this air-mass is transported to the Levant

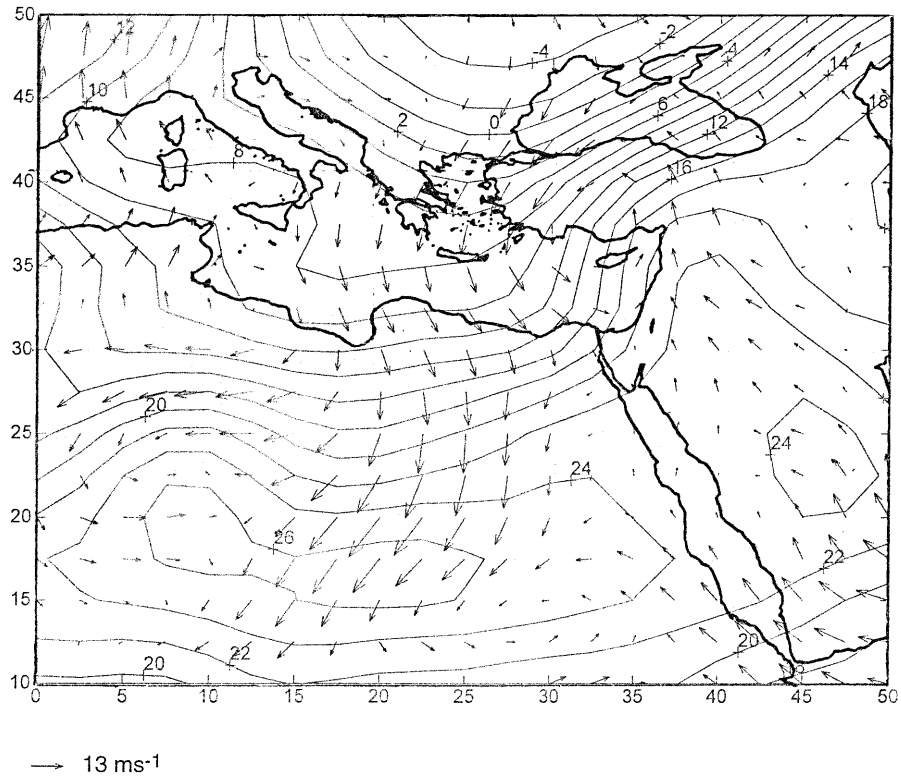

Fig. 6. 850 hPa isotherms (with 2 °C interval) and wind vectors for 17 Oct 1997 1800 UTC, indicating cold advection over Israel

the mesoscale systems that have evolved under the atmospheric conditions described above.

During the afternoon of Oct 17 a cloud system of 50–100 km in diameter advanced from Sinai into the central Negev (Fig. 9), in line with the prevailing south-south-westerly wind between 850–200 hPa (Fig. 4b). The system moved at 30–40 km h^{-1} (see isochrones in Fig. 11). Subse-

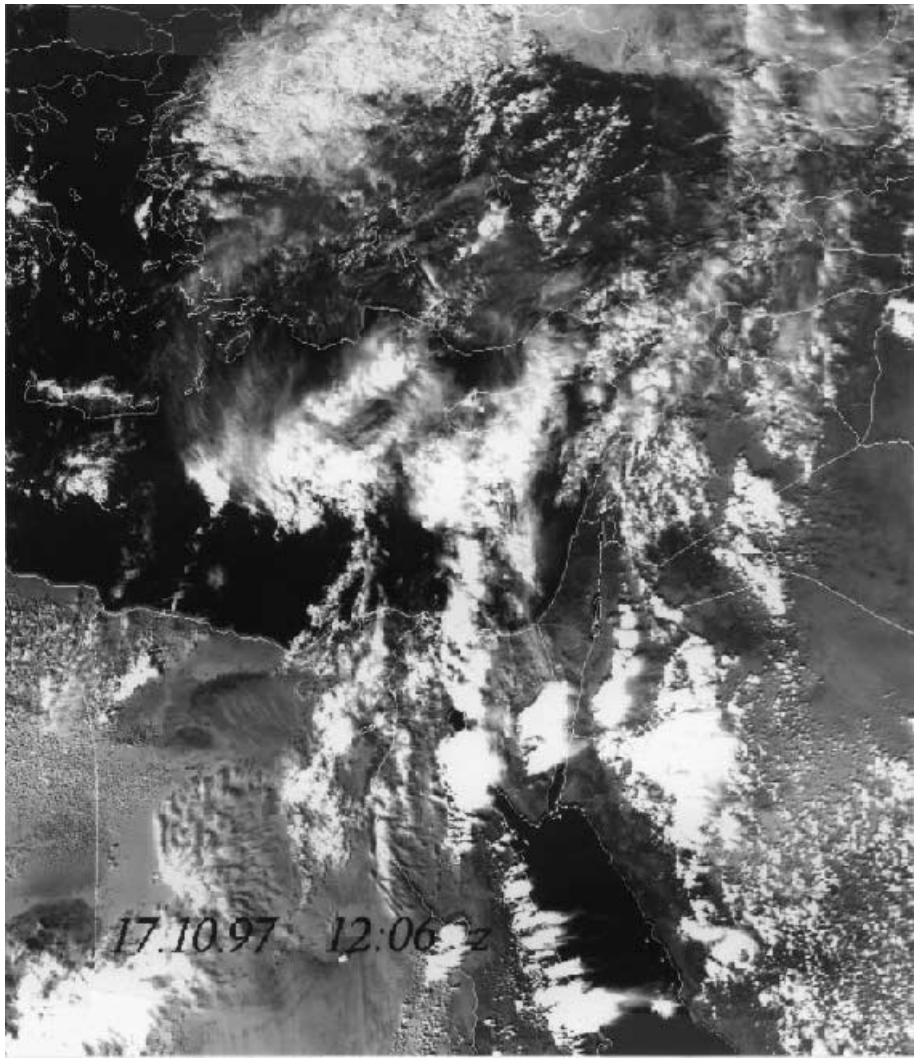

Fig. 7. NOAA satellite visible picture for 1206 UTC 17 Oct 1997, showing the convective cells which developed quickly, particularly over the mountain ridges along the Red Sea coast

quently, while expanding and changing shape, the system accelerated to 45 km h^{-1} and moved farther northward along Israel up to Lebanon till 2200 UTC. The system spread light to moderate rain (2–6 mm) over most of the country (Fig. 12). During its passage over the northern Negev and the Judean Hills an approximate 1.5 h long backing of winds from north-west to south-west was observed, together with an 40 min long intensification from less than 5 to over 10 m s^{-1} (e.g. Fig. 13).

While light rains were observed over most of the country, intense smaller convective cells of less than 10 km in diameter, accompanied by thunder, gale, and heavy showers, were taking place within that system over abrupt topographical features (Fig. 14). This occurred first in the south of the country (the Negev) and Sinai, then along the Rift Valley in the east. The latter occurred along the 600–1000 m high eastern slopes of the central mountain ranges of Israel, overlooking the Dead Sea, and the Jordan Valley. In large parts these slopes consist of a series of massive escarpments formed by the recent geological downfaulting along the rift walls. The combination of small, intense convective elements (Fig. 14), embedded in a larger stratiform cloud of 100 km scale (Fig. 9), fits the definition of a Mesoscale Convective System, MCS (Maddox, 1980; Ray, 1986).

Following below is a more detailed scrutiny of the smaller scale convective elements as they developed within the system during its 9-h passage northwards over Israel.

- At 1300–1400 UTC extreme flooding occurred south of Eilat and in the upper tributaries of the Paran watershed (Fig. 1).

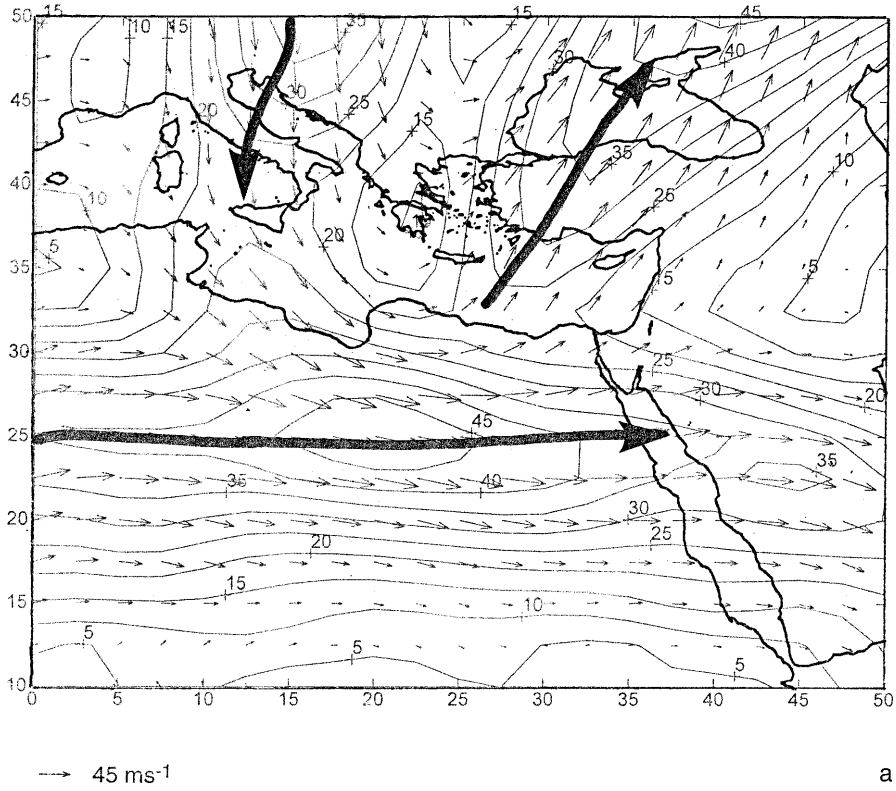

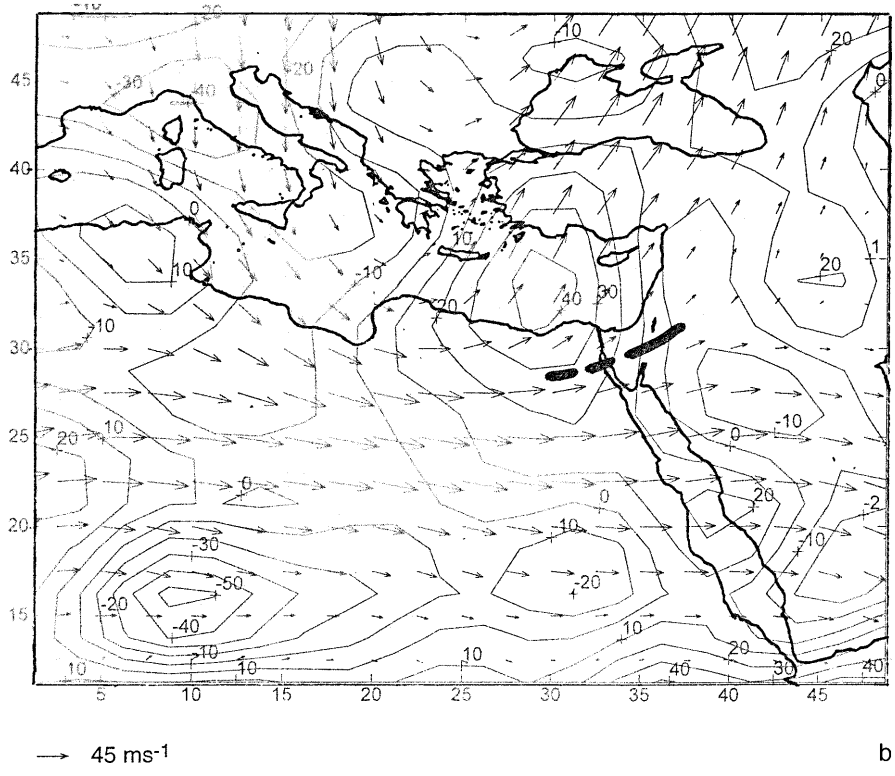

Fig. 8. 200 hPa wind field for 1200 UTC 17 Oct 1997; (**a**) wind speed (isotachs with $5\,\mathrm{m\,s^{-1}}$ intervals) and wind vectors. Heavy arrows represent main jet streaks. (**b**) divergence and wind vectors (divergence isopleth intervals of $10 \times 10^{-6}\,\mathrm{s^{-1}}$). Heavy dashed line represents the line of diffluence over Sinai

- Between 1500–1600 UTC precipitating convective elements within the MCS extended from west-south-west to east-north-east over the 1000 m high central Negev (Fig. 14). Three distinct elements were moving northward and diverging from each other.
- At 1700 UTC a precipitating convective element was affecting the lowlands 20 km

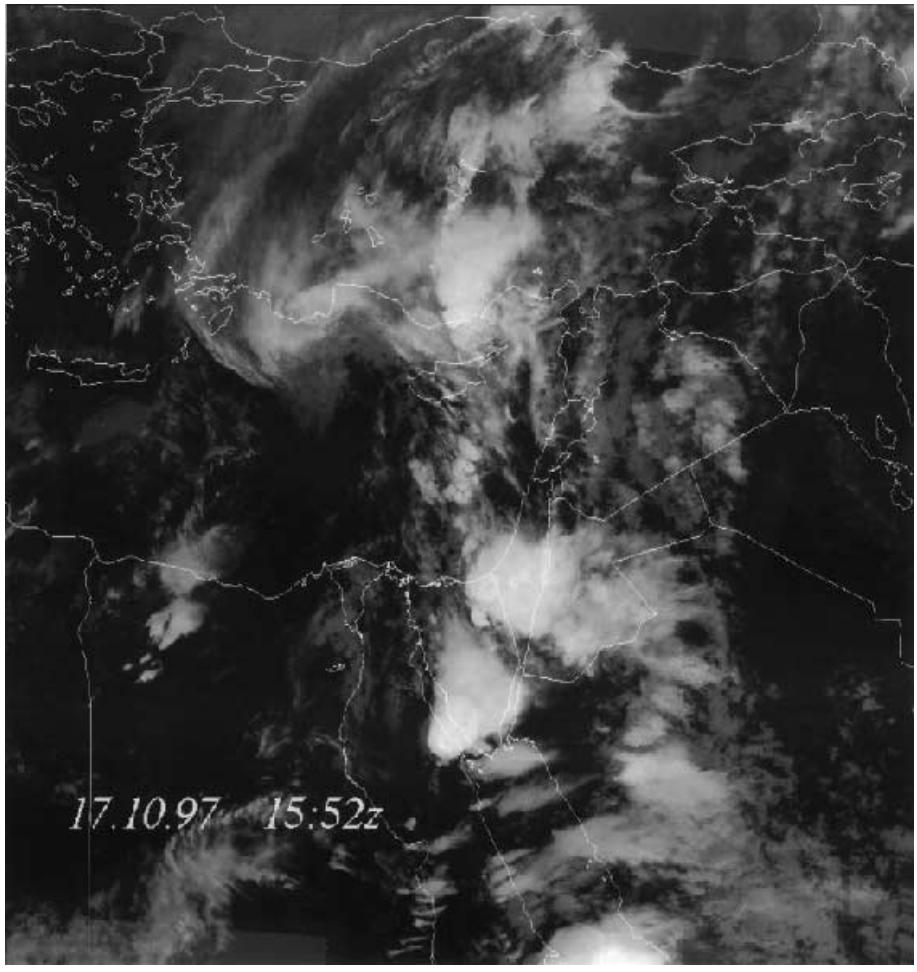

Fig. 9. NOAA satellite IR picture for 1552 UTC 17 Oct 1997, showing the diffluent winds aloft as reflected by the drifting of cloud tops between west over Saudi-Arabia and south-south-west over Sinai

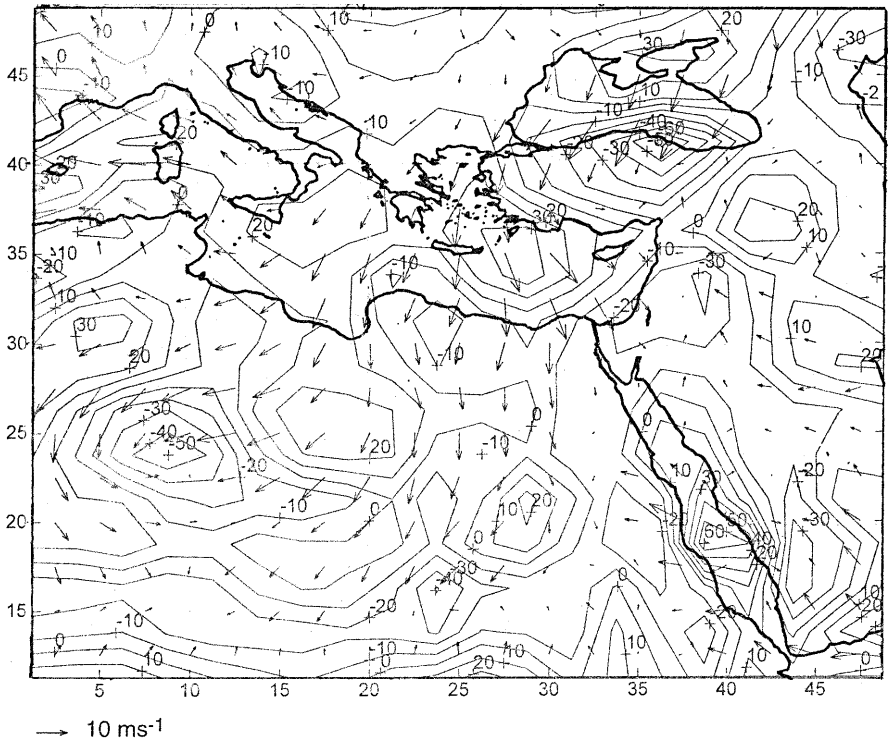

Fig. 10. Sea level divergence field (isopleths with $10 \times 10^{-6}\,s^{-1}$ interval) and wind vectors for 1200 UTC 17 Oct 1997, showing the convergent flow (negative values) over Israel and Jordan due to confluence of weak south-easterly flow and north-north-west flow

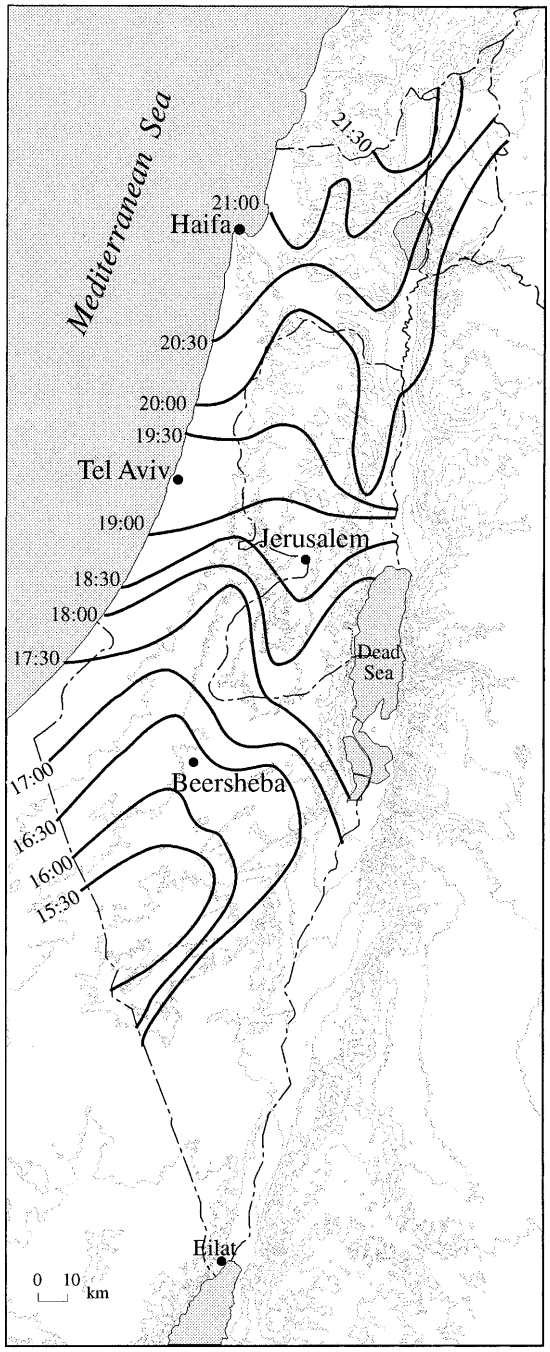

Fig. 11. Isochrones of the progression of the precipitating elements of the MCS, steered by the south-south-western flow aloft, 17 October 1997 1530–2130 UTC. Isochrones denote the time by which 15% of the daily total was accumulated

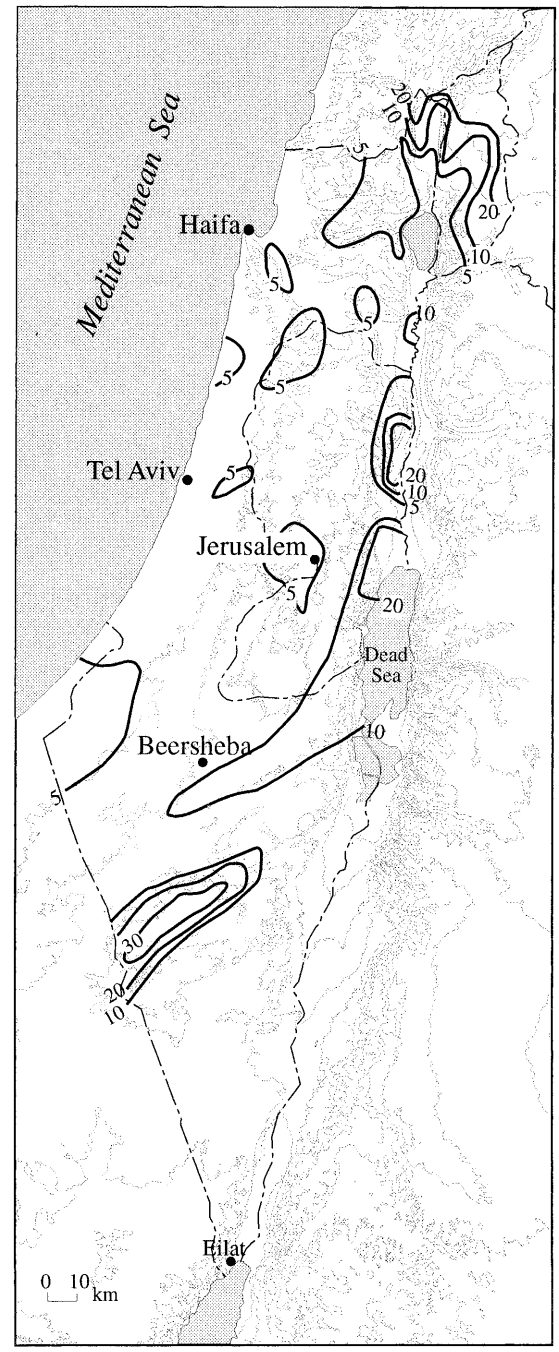

Fig. 12. Rainfall totals over Israel (mm) accumulated during the passage of the MCS, 17 Oct 1997 1530–2130 UTC

west of Beersheba (Fig. 14). Simultaneously, other elongated twin clusters and some smaller elements were intensifying over the south-east and east facing slopes in the lee of the southernmost outliers of the Judean Hills.

By 1800 UTC, as the system was moving farther north, the western element had disintegrated, whereas the eastern one intensified and moved northward. Intense convective activity associated with the latter raged to the east of the

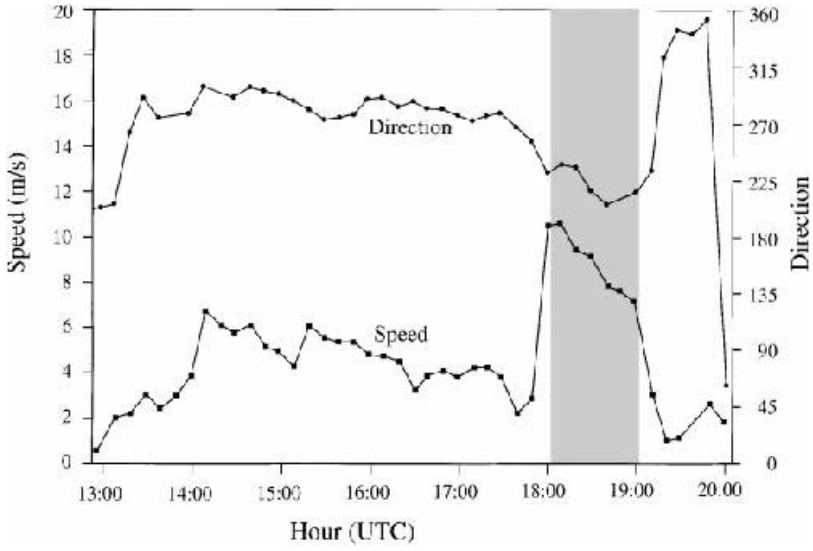

Fig. 13. Temporal variation of wind direction (•) and speed (■), 17 October 1997, in Jerusalem. Vertical shaded column delineates the period during which a backing and intensification of the wind persisted

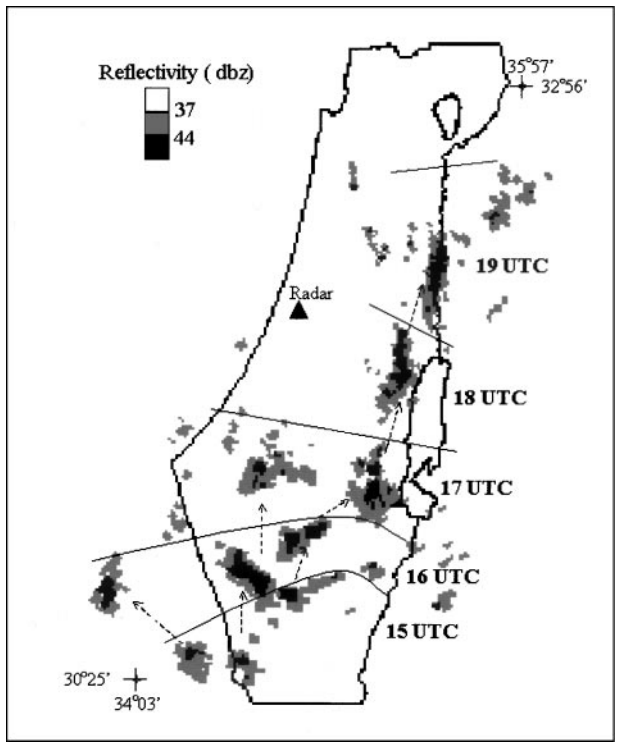

Fig. 14. Superposition of hourly radar reflectivity scans (dbz), 17 October 1997, 1500–2000 UTC showing the divergence (or splitting) of cells over the central Negev (1500–1700 UTC) and the intensification of elements to the lee of the Judean Hills (1700–1900 UTC). Dashed arrows represent the assumed paths of cells

hilly region, by now within a narrow 30 km long north-south oriented strip (Fig. 14) of high-intensity showers exceeding 110 mm h^{-1}. The narrow strip extended over the eastern slopes of the Judean Hills and was translating northwards, in tandem with the MCS and with an associated backing and intensification of the winds over that region for 1.5–2 hrs (Fig. 13). A similar change in the wind was observed a little earlier on a raft off the coast near Ein Gedi from a north-easterly to a north-westerly direction. The fact that heavy rain on that evening was strictly confined to the slopes only is also evident from hydrologic reports. Thus, although only very light rains were observed along the ridges of the Judean Hills and west of them (Fig. 12), severe flooding occurred that evening in all wadies draining the eastern slopes into the Rift Valley (Novak, 1998, Tb.5.3.1).

- Around 1900 UTC, the active strip was already situated above the more moderate eastern slopes of the Samarian Hills, lacking rocky escarpments. This may have contributed to the somewhat more diffuse appearance of the strip, as well as its slight drifting eastwards, to the lowest part of the slope. Still, over 40 mm of high-intensity rainfall was observed in that area at Argaman, 35 km north of Jericho.
- After 1900 UTC, as the system was moving over the much lower hills of northern Samaria and the Lower Galilee, the winds receded and veered back to a north-northeastern direction, and rainfall in the respective parts of the Rift Valley ceased. Yet, gusty winds and thunder were still reported at a few sites, along the relatively warm Rift Valley, including Lake Tiberias.

- Between 2000–2100 UTC thunderstorms were affecting the steep 800–900 m high slopes of the northern Hula Valley (on both sides) yielding 20–25 mm of rain with a recorded intensity of 140 mm h^{-1} at places (e.g. Kfar Gil'adi), accompanied by southerly winds of 10–15 m s^{-1}. By 2200 UTC the MCS had already moved into Lebanon. At the same time, another system, to the south of the former, crossed the southern Negev northward, yielding 16 mm of rain in Eilat, (half of the annual average there!) within 10 minutes, which caused a local flood over the lower part of the town.

After midnight (Oct 18, 0000 UTC) the storm activity faded out. The satellite image from that time (not shown) indicates that Egypt, Sinai, Israel and southern Lebanon were almost free of active cloudiness. This may have been caused by both the nocturnal stabilization affecting convection in general, and by a significant decrease in the 200 hPa upper divergence from over 25×10^{-6} s^{-1} on Oct 17, 1200 UTC (Fig. 8b) to less than 10×10^{-6} s^{-1} (not shown).

5. Phase II: Activation of a high instability by a cold front (Oct 18)

In the morning hours of October 18 1997 the PJ moved slightly eastwards from its position on the previous day shown in Fig. 8a, and it now extended above Israel. However, the Levant region still retained the same position relative to both jets, i.e., to the left of the STJ exit and to the right of the PJ entrance. The surface charts show an eastward shift of the Red Sea trough with a newly formed cyclone above south Turkey and Cyprus (Fig. 15). The latter was accompanied by an advance of the trough at the 500 hPa level (mentioned in Section 4.1) toward the eastern Mediterranean and with a baroclinic low at 850 hPa over Turkey, as implied by the wind vectors in Fig. 16. The motion of the 500 hPa trough was at a rate of 4° longitude per 24 h, i.e., from 24° to 28° E between October 17 and 18, 12 UTC (500 hPa maps not shown). However, convective elements were still affecting parts of the region, as described below. Unlike in Phase I, they were now organized both in time and space, by an approaching cold front.

In the early morning hours of Oct 18 isolated Cumulonimbi were forming in the south-east Mediterranean region, with well-developed anvils (Fig. 17). The one near Gaza stands out with its very regular, well-defined shape, to which the convergent land breeze along the concave coast of Israel and Sinai suggested by Neumann, 1977. Concurrent winds at Gaza and other stations in the region were, indeed, south-easterly with a speed of 2–3 m s^{-1}. A sequence of radar scans (not shown) indicates a subsequent north-eastward propagation of this cloud and a drifting of its anvil which thus attained an elongated shape. While extending further north, between 0500–0800 UTC, the latter was spreading light rains over the coastal plain.

Between 0900–1100 UTC, a series of circular thunderstorm clusters crossed the coast line toward the northern Negev. As they moved farther

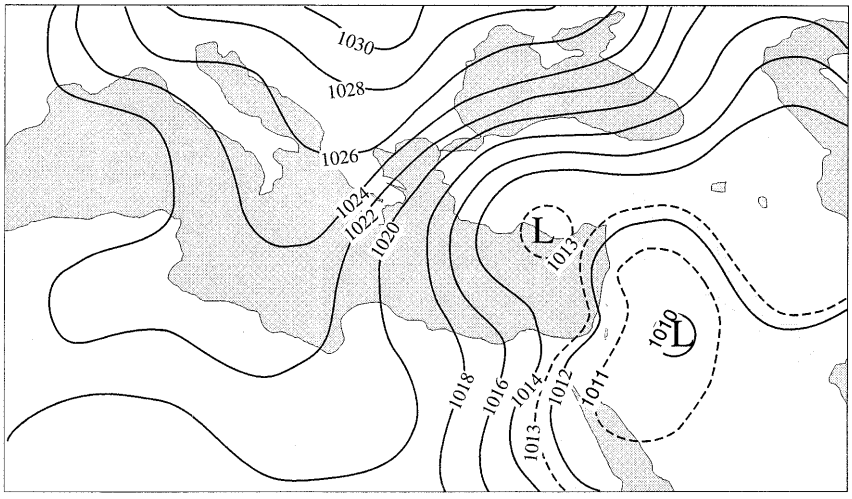

Fig. 15. Sea level pressure (with 2 hPa interval) for 18 Oct 0600 UTC, showing the eastward shift of the Red Sea trough and the formation of a Cyprus low

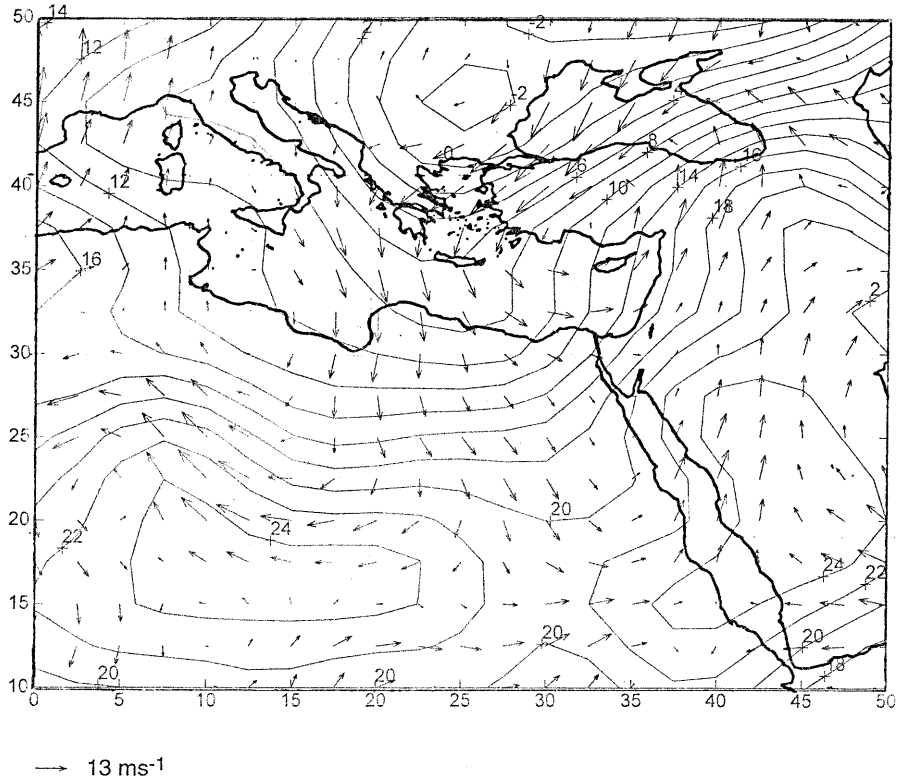

Fig. 16. 850 hPa temperatures (with 2 °C interval) and wind vectors for 18 Oct 1997 1200 UTC

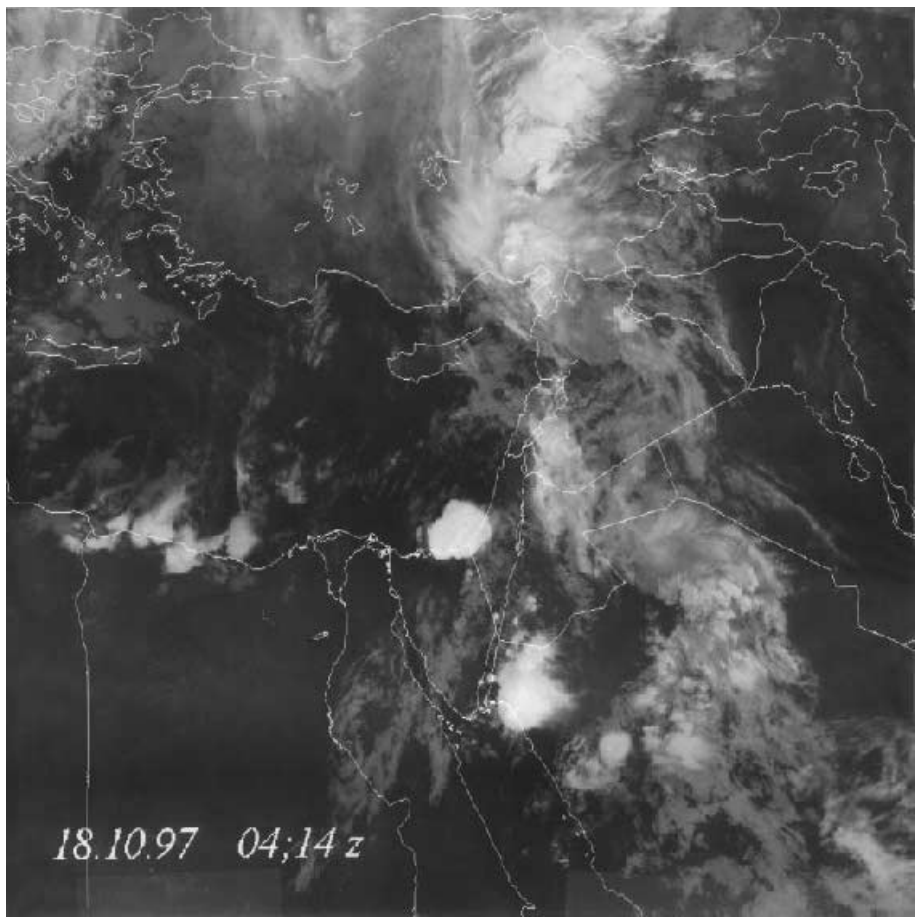

Fig. 17. NOAA satellite IR picture for 0414 UTC 18 Oct 1997, showing the isolated Cumulonimbi over the southeastern Mediterranean

inland toward noon, they were still developing and intensifying. A sequence of radar scans (not shown) indicates that these clouds were gradually organizing into a thick line with 200–020° orientation, while advancing inland, toward the east. It included several extremely active elements extending south-westward over the northern Negev. One of these hit Beersheba in the northern Negev at 1100 UTC, and resulted in huge hailstones (2.5–5.0 cm diameter) and severe showers (20 mm with intensity up to 216 mm h^{-1} for 2 successive minutes) accompanied by gusts of 27 m s^{-1}. Extreme floods were formed over catchments that were hit by these showers (e.g. 160 m^3 s^{-1} in a 36 km^2 watershed, the highest discharge measured there in the last 50 years).

By 1155 UTC the line of storms mentioned was already incorporated in the wide thick cloud sheet with a sharp western edge shown in Fig. 18. The latter reflects a cold front over the Levant, that may be inferred also from the 850 hPa temperature field in Fig. 16. The location and orientation of the front coincide with those of the concurrent position of the PJ mentioned above.

While moving within a still highly unstable environment, the front activated deep convection, manifested in Fig. 19 as a line of heavy thunderstorms advancing over the Judean Hills. As the front was moving eastward, the precipitating elements approaching the Dead Sea and the Jordan Valley did not disintegrate over the 1000 m high lee-side slopes, as it is common in 'ordinary' rainstorms affecting this area (see Section 6.1 below). Figure 19 shows quite clearly that these elements may even have expanded and intensified after passing the divide. This is supported by daily rainfall totals of 15–20 mm at Ein Gedi near the Dead Sea (Novak, 1998, Table 5.3.2) as compared to 14–18 mm on the ridge south of Hebron, (not shown) directly upwind of Ein Gedi. In addition,

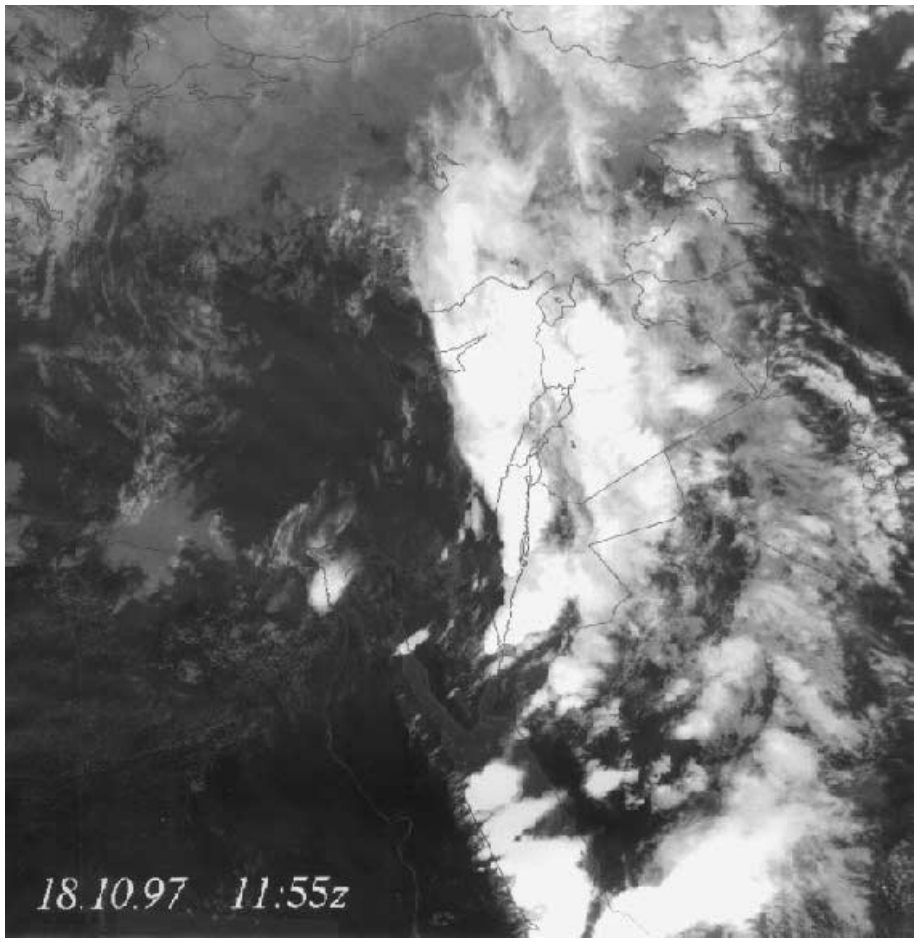

Fig. 18. NOAA satellite IR picture for 1155 UTC 18 Oct 1997, showing a distinct frontal structure over the Levant

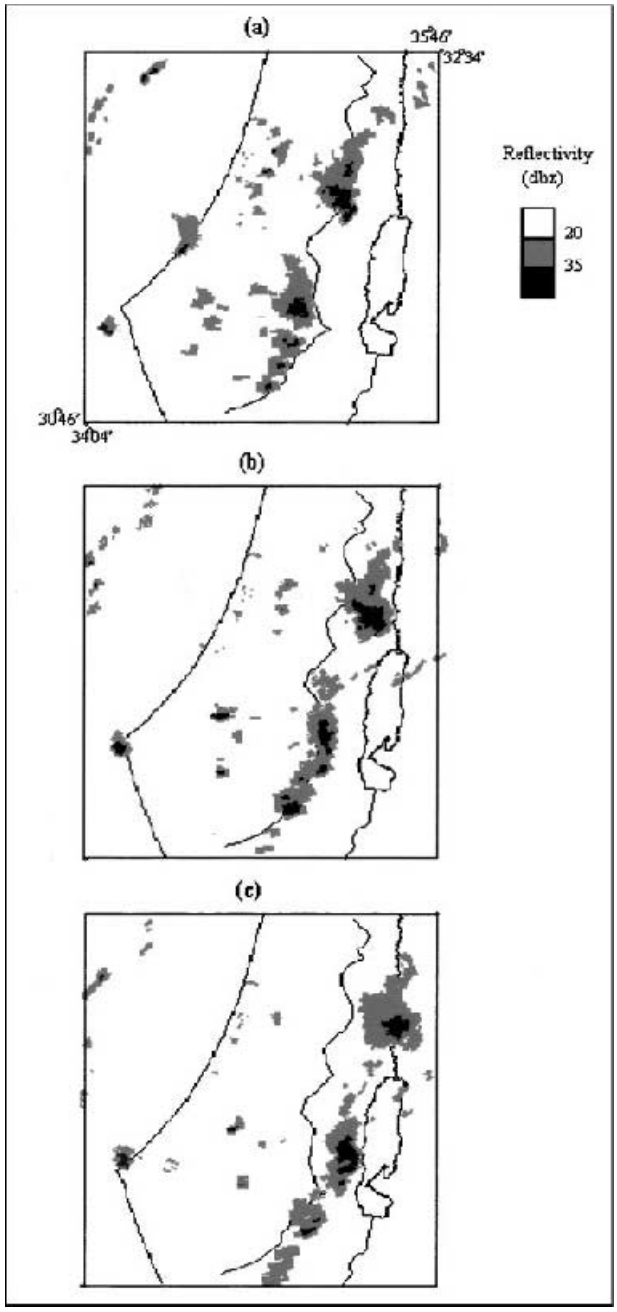

Fig. 19. Selected radar reflectivity scans for (**a**) 1101 UTC (**b**) 1121 UTC and (**c**) 1136 UTC 18 Oct 1997. The main water divide is denoted (after Novak 1998)

resulting floods in the Dead Sea area were even heavier than in Phase I (Novak, 1998, Fig. 5.3.3 and p. 72).

The passage of the above front and a farther eastward movement of the Red Sea trough denote a transition to the more common extra-tropical Cyprus low that developed over the Eastern Mediterranean with a new position of the upper-level trough at 500 hPa (not shown). As such, that ensuing phase is beyond the scope of this study.

6. Discussion

This study deals with a major autumn rainstorm that affected the ME on 17–19 October 1997, associated with the Red Sea trough. The storm was characterized by its extensive coverage (Egypt, Israel and Jordan simultaneously), extreme rain intensities with huge hailstones and gales that resulted in casualties and damages caused by floods. The paper describes its both the synoptic-scale processes and the phenomenological aspects.

Prior to the formation and intensification of the storm, a preexisting Red Sea trough transported hot air toward the ME in the lower levels (Fig. 3a,b), establishing conditional instability there (Fig. 4a,b). Subsequently a mid-latitude upper trough from Greece approached the region, accompanied by an intensification of the STJ over Africa and a formation of a PJ over Turkey (Fig. 8a). The ME was then situated simultaneously to the left of the STJ exit and to the right of the PJ entrance, implying near tropopause divergence. An increase in relative humidity within the mid-troposphere under conditional instability (compare Fig. 4a and 4b), along with the synoptic-scale forcing, stimulated intense convection.

At its first phase the storm had the character of tropical convection, with high temperatures. During that phase local topography played a major role in this context, as is specified in subsection 6.1 below. At the second phase convective cloudiness still prevailed, only that it was now organized along a cold front that swept Israel that day (Figs. 16, 18, 19), which subsequently led to the transformation of the storm into a mid-latitude baroclinic system.

6.1 Convection and surface effects

During the entire storm (especially in phase I), the spatial and temporal patterns of the intense convective activity offer evidence linking it to external mesoscale factors that apparently enhanced that activity. This is in agreement with Doswell et al. (1996) who emphasized the role of mesoscale terrain features in the above context. The effect of topography on mesoscale convective systems over the region studied here was

also stressed by Greenbaum et al. (1998) who analyzed a high-magnitude rainstorm and flood that took place on October 1991. Here are several examples:

Radar scans from 17 October, around 1500–1600 UTC, clearly reflects the effect of prominent ridges and escarpments in the 800–1000 m high central Negev Mountains, in the initiation of convective elements (Fig. 14). Later, between 1700–1900 UTC, the development of intense convection was restricted to the abrupt western rim of the Rift Valley (see Sec. 4.2 above). The 30 km long strip of convective activity that was translating over these slopes around 1800–1900 UTC apparently delimits the area within which the fresh south-westerly flow associated with the MCS (Fig. 13) could be driving a turbulent surface flow which – in turn – may have contributed to trigger convection over the precipitous lee-side slopes. Before the invasion of the above winds, easterly surface winds of 4–5 m s^{-1} were observed at the Dead Sea, flowing toward the escarpment. An easterly surface flow along with the passage of winds with a westerly component blowing across a steep mountain ridge with a north-south orientation was found by Carlson et al. (1983) to be an important contributor to the stimulation of convection on the lee-side slopes.

Deep convection was again enhanced along the same line on the following day, with the convective elements strung out along an advancing cold front (see Sec. 5). The persistence of deep convection observed on that day during the descent over the 1000–1400 m high lee-side slopes is very unusual under normal frontal situations. Hence it may suggest the recurrence of a mechanism in which, under a westerly flow, an already existing intense regional instability can be locally released over these lee side escarpments. A numerical study of orogenic MCSs development (Tripoli and Cotton, 1989) and an observational study of convective storms interacting with major topographic features (Garstang et al., 1987) support this hypothesis. Situations in which rain intensities over the above mentioned escarpments were significantly higher than in their surroundings have been observed in past (e.g., 17 Oct 1987, Margalit, personal communication).

The divergence (or splitting) of convective elements from each other that was observed over the central Negev on October 17, 1500–1600 UTC (Fig. 14) may have resulted from the steering of the diffluating jets aloft (Fig. 8a). However, a similar pattern of evolution has been observed in that area in a previous rainstorm (December 1993, Margalit, personal communication). Both events may suggest that beside the synoptic scale forcing the abrupt topographic features in that region also have played a role in this type of unique evolution.

Topography also seems to have played a role in the enhancement of convection later that evening over the Galilee, at northern Israel, 2000–2100 UTC. The southerly flow along the Hula Valley was ascending with the slope of the valley bottom, but even more due to the convergence forced by the escarpments encroaching on both sides of the valley. These two effects may explain the extreme rain intensity recorded there (Sec. 4.2). Thus, the present analysis offers evidence for three different mechanisms by which abrupt topography may enhance deep convection: Upslope forcing, convergent channeling into a deep rift valley and a less-well understood mechanism taking place over massive lee-side escarpments.

6.2 Synoptic scale factors

The storm studied here involves elements from a variety of climatic regimes, i.e., tropical elements (Red Sea trough and tropical moisture), the subtropical jet and mid-latitudinal systems (PJ, Cyprus cyclone and cold front).

Krichak and Alpert (1998) analyzed numerically a severe autumn rainstorm that took place over the ME in November 1994 under the influence of a Red Sea trough, and proposed the following sequential events: (1) Enhanced moist advection from the Arabian Sea toward equatorial Africa that stimulates convection there. As a result, (2) the STJ over the Red Sea is intensified, thus, (3) enhancing the Red Sea trough, which in turn, (4) transports moist tropical air-mass from the Arabian sea north-westward, toward the ME. Finally, (5) when cyclogenesis takes place over the ME both the Red Sea trough and the STJ weakens and moist air masses from the Arabian Sea are again directed toward tropical Africa.

The analysis of the above storm confirms the general evolution as proposed by Krichak and Alpert (1998), in particular the existence of stages (2), (3) and (5). Concerning stage (4), i.e., moisture transport toward the ME, the situation in the

present case is different. Moisture does not originate from the south east, but rather from south west as reflected in Fig. 5. In this respect, the case dealt with here is more similar to those studied by Leguy et al. (1983), Sasson (1990) and Zangvil and Isakson (1995) in which moisture transport originated from west Africa.

Unlike the case studied by Krichack and Alpert (1998) we suggest here that the approach of a mid-latitude upper-trough toward the ME may also have contributed to the development and intensification of the storm in the following ways:

- The enhanced south-western flow ahead of the trough at the middle levels may have transported moisture from western equatorial Africa to the ME (Fig. 5).
- The PJ ahead of the trough over Turkey contributed to the upper-level divergence over the ME, situated underneath the right side of its entrance (Fig. 8a,b). The divergence may be further enhanced due to a coincidence with the divergence imparted on the left side of the STJ exit over the ME, where along-stream deceleration of the wind took place (Fig. 8a). A co-location of two divergence centers associated with two distinct jets was suggested by Uccellini and Kocin (1987) as the background for an explosive cyclogenesis that took place over the eastern coast of the United States, regardless whether the jets are parallel to each other (as in their case) or almost perpendicular to each other, as in the present case.
- The cold front associated with the developing Mediterranean cyclone on 18 October contributed an additional drive for convection (Figs. 16, 18, 19).
- The cool air surge at the lower levels over Greece (e.g. Fig. 6) enhanced the zonal temperature gradient along northern Africa. Thermal balance implies that this would enhance the STJ there. Such an intensification is found to initiate the development of the Red Sea trough (Krichak et al., 1997b) and the ageostrophic effects, such as the divergence to the left of its exit, right over the ME (Fig. 8b).

In addition, instability is enhanced when an approaching mid-latitude trough causes upper-level cooling, while the lower levels remain hot by the influence of a Red Sea trough (El-Fandi, 1948).

Some other effects of a mid-latitude trough on autumn rainstorms have been observed. In a previous storm that occurred over the ME on 17 October 1987 a mid-latitude trough penetrated into the subtropics, so that the STJ over north-eastern Africa curved cyclonically, unlike in the above storm. As a result a divergence center was found at the inflection region of the jet ahead of the trough, over southern Israel, presumably contributing to the intensity of the rainstorm.

The mean 500 hPa flow field for October 1997 (NOAA, 1998) shows a distinct trough extending from Scandinavia southward via central Europe down to Greece. At the center of this region the monthly negative anomalies exceeded 15 m. Moreover, negative anomalies were observed there on 70% of the days at that month. In other words, in October 1997 the eastern part of the Mediterranean was recurrently situated under the front edge of an upper-level trough. This may suggest that this autumn rainstorm was not an incidental event, but rather may reflect a cumulative effect of longer term systems, on the order of a month.

6.3 Seasonality of the Red Sea trough over the ME

The connection between the STJ and the development of the Red Sea trough (Krichak et al., 1997b), together with the seasonal variations in the proximity of the African Monsoon to the ME, may explain the tendency of the Red Sea trough to develop in the autumn. The African Monsoon is at its closest position to the ME in October as compared to the winter, when it moves farther to the south (Barry and Chorley, 1998), so the winter season is unfavorable for such development. Concerning the STJ, in summer it is positioned over Turkey, thus too far from the Red Sea, where it may affect the Red Sea trough. In the transition from September to October the STJ is displaced southwards, from the 36° N latitude (over Syria, north Iraq and north Iran) to 28–29° N (see also, e.g., Lahey et al., 1960), where it may initiate the development of a Red Sea trough.

Being a source of potential damage, a timely and reliable forecasting of rainstorms associated with the Red Sea trough is required. The above findings and hypotheses point at several frameworks in which improvement of forecasting skill can be achieved. For example, the hypothesized linkage between the intensity of the storm and the

approach of a mid-latitude trough toward the ME suggests that when a Red Sea trough extends over the region, the approaching trough should be considered as an alarm. Further, if specific topographical effects, as noted here, prove to be consistent in other events they may enable the forecaster to point at potential sites susceptible to floods, e.g., expected westerly winds over the Judean Hills may indicate the likelihood of a flood occurrence over their eastern escarpments. The above discussion implies that further effort is required to investigate such rainstorms in general and the topographical and other surface effects in particular.

Acknowledgements

This research and development was supported in part by funds provided to the International Arid Lands Consortium (IALC) by the USDA Forest Service and by the USDA Cooperative State Research, Education, and Extension Service. The IALC was established in 1990 as a means to promote research, demonstrations, and training applied to development, management, restoration, and reclamation of arid and semiarid lands in North America, the Middle East, and elsewhere in world. The authors are grateful to the Israeli Meteorological Service for the rain gauge recordings; to the Electro-Mechanical Service Ltd. and the Cloud and Precipitation Physics Laboratory of the Tel Aviv University for the radar reflectivity data; to H. Lavee from Bar Ilan University; Israel, for the rain intensity data for Kalia, to A. Hecht of the Israel Oceanographic and Limnological Research Ltd. for the Dead Sea Buoy data as well as to A. Schick, R. Garti and H. Ben David-Novak for their useful comments and description of the damages caused by the floods during the rainstorm. Special thanks are due to Michal Kidron from the Cartographic Lab. at the Dept. of Geography at the Hebrew University of Jerusalem for her assistance in preparation of the figures.

References

Air Ministry Meteorological Office (1962) Weather in the Mediterranean, Vol. 1, 362 pp

Ashbel D (1938) Great floods in Sinai peninsula, Palestine, Syria and the Syrian desert, and the influence of the Red Sea on their formation. Quart J Roy Meteor Soc 64: 635–639

Bar-Lavy B, Margalit A, Sharon D (1977) Desert rainfall patterns associated with the Red Sea trough. Int Conf on the Meteorology of Semi-Arid Zones. 31.10–4.11.77, Tel-Aviv

Barry RG, Chorley RJ (1998) The African Monsoon. Atmosphere Weather and Climate, Routledge, Seventh Edition, 409 pp

Carlson TN, Benjamin SG, Forbes GS, Li YF (1983) Elevated mixed layers in the regional severe storm environment: Conceptual model and case studies. Mon Wea Rev 111: 1453–1473

Dayan U, Sharon D (1980) Meteorological parameters for discriminating between widespread and spotty storms in the Negev. Isr J Earth Sciences 29(4): 253–256

Doswell III CA, Brooks HE, Maddox RA (1996) Flash flood forecasting: an ingredients-based methodology. Wea Forecasting 11: 560–581

El-Fandi MG (1948) The effect of the Sudan Monsoon Low on the development of thundery conditions in Egypt, Palestine and Syria. Quart J Roy Meteor Soc 74: 31–38

Garstang M, Kelbe BE, Emmitt GD, London WB (1987) Generation of convective storms over the escarpment of north-eastern South Africa. Mon Wea Rev 115: 429–443

Greenbaum N, Margalit A, Schick AP, Sharon D, Baker VR (1998) A high magnitude storm and flood in a hyperarid catchment, Nahal Zin, Negev Desert, Israel. Hydrol Process 12: 1–23

Hayward DF, Oguntoyimbo JS (1987) The Climatology of West Africa. London: Hutchinson, 271 pp

Israel Meteorological Service (1983) Vol. 1 – Averages of temperatures and relative humidity (1964–1979), Series A (Meteorological Notes), No 41

Kalnay E, Kanamitsu M, Kistler R, Collins W, Deaven D, Gandin L, Iredell M, Saha S, White G, Woollen J, Zhu Y, Chelliah M, Ebisuzaki W, Higgins W, Janowiak J, Mo KC, Ropelewski C, Wang J, Leetmaa A, Reynolds R, Jenne R, Joseph D (1996) The NCEP/NCAR 40-year reanalysis project. Bull Amer Meteor Soc 77(3): 437–471

Kelway PS, Herbert SI (1969) Short term rainfall analysis. Weather 24: 342–354

Krichak SO, Alpert P, Krishnamurti TN (1997a) Interaction of topography and tropospheric flow – A possible generator for the Red Sea trough? Meteorol Atmos Phys 63: 149–158

Krichak SO, Alpert P, Krishnamurti TN (1997b) Red Sea trough/cyclone development – Numerical investigation. Meteorol Atmos Phys 63: 159–169

Krichak SO, Alpert P (1998) Role of large scale moist dynamics in November 1–5, 1994: Hazardous Mediterranean Weather. J Geophys Res 103: 19,453–19,468

Lahey JF, Bryson RA, Corzine HA, Hutchins CW (1960) Atlas of 300 mb wind characteristics for the northern hemisphere. The University of Wisconsin Press

Leguy C, Rindsberger M, Zangvil A, Issar A, Gat JR (1983) The relation between the oxygen-18 and deuterium content of rain water in the Negev Desert and air mass trajectories. Isot Geosci 1: 205–218

Maddox RA (1980) Mesoscale convective complexes. Bull Amer Meteor Soc 61: 1374–1387

Morin J, Sharon D (1993) Rainfall intensity analysis as a tool for water resources planning. Curr Iss Hydrol, Zurich Geogr Scripts 53: 52–59

Morin J, Sharon D, Rubin S (1998) Rainfall intensity in Israel, Selected Stations, Research Report 1/94 (Revised Version). Israel Meteorological Service, The Hebrew University of and the Ministry of Agriculture, Bet Dagan, 149 pp

Neumann J (1977) On the rotation of the direction of sea and land breezes. J Atmos Sci 34: 1913–1917

NOAA (1998) Climate Diagnostic Bulletin, October 1997, Climate Prediction Center, Near Real-Time Analyses Ocean/Atmosphere, US Department of Commerce, National Oceanic and Atmospheric Administration, National Weather Service, National Centers for Environmental Prediction

Novak H (1998) Modern and Holocene debris – flows along the western escarpment of the Dead Sea. (Hebrew) MSc Thesis in Physical Geography, The Hebrew University of Jerusalem

Ray PS (1986) Mesoscale Meteorology and Forecasting. Amer Meteor Soc, 793 pp

Ronberg B (1985) An objective weather typing system for Israel: a synoptic climatological study. PhD Thesis, The Hebrew University of Jerusalem

Sadler JC (1975) The Monsoon circulation and cloudiness over the GATE area. Mon Wea Rev 103: 369–387

Sasson A (1990) Connection between synoptic characteristics and atmospheric moisture field, and major rain storms over Israel. (Hebrew) MA Thesis, Ben-Gurion University of the Negev, Israel

Shaia JS, Siles G (1972) Upper air data for some stations in the Middle-East (1957–1966) Series A: Meteorological Notes No 27. Israel Meteorological Service

Sharon D (1974) The spatial pattern of convective rainfall in Sukumaland, Tanzania – A statistical analysis. Arch Met Geoph Biokl, Ser B 22: 201–218

Sharon D (1981) The distribution in space of local rainfall in the Namib Desert. Int J Climatol 1: 69–75

Sharon D, Kutiel H (1986) The distribution of rainfall intensity in Israel, its regional and seasonal variations and its climatological evaluation. Int J Climatol 6: 277–291

Tripoli GJ, Cotton WR (1989) Numerical study of an observed orogenic mesoscale convection system, Part 1: Simulated genesis and comparison with observations. Mon Wea Rev 117: 273–313

Uccellini LW, Kocin PJ (1987) The interaction of jet – streak circulations during heavy snow events along the east coast of United States. Wea Forecasting 2: 289–308

Zangvil A, Isakson A (1995) Structure of the water vapor field associated with an early spring rainstorm over the eastern Mediterranean. Isr J Earth Sci 44: 159–168

Authors' addresses: Prof. Uri Dayan (e-mail: msudayan @mscc.huji.ac.il), The Department of Geography, The Hebrew University of Jerusalem, Mt. Scopus, Jerusalem 91905, Israel. Baruch Ziv, The Open University of Israel, Tel Aviv. Adina Margalit, Efrat Morin, David Sharon, Earth Science Institute, The Hebrew University of Jerusalem, Israel.